J. Am. Chem. Soc. **1980**, *102*, 7080–7087

Chiroptical Properties of Proteins. 1. Near-Ultraviolet Circular Dichroism of Ribonuclease S†

Warren J. Goux and Thomas M. Hooker, Jr.*

Contribution from the Department of Chemistry, University of California, Santa Barbara, California 93106. *Received December 26, 1979*

Abstract: The near-ultraviolet circular dichroism spectrum of ribonuclease S has been investigated. Theoretical calculations, based upon the X-ray crystal structure of the enzyme, have been carried out by means of a matrix formalism which includes the configuration interaction of excited states. The results of the calculations indicate that the features observed in the near-ultraviolet circular dichroism spectra of this protein arise from electronic transitions associated with the tyrosine and cystine chromophores. The optical activity of these transitions arises primarily from coupling interactions involving similar transitions on other residues and nearby amide transitions. The fact that the theoretical calculations, which were based upon coordinates derived from the crystalline state, show reasonable agreement with experimental circular dichroism data determined in solution is good evidence that the structures which exist in these two states must be quite similar.

Introduction

The development of physical and chemical techniques suitable for probing the conformation of molecules in solution has long been the object of considerable effort by numerous investigators. Recent evidence that there may be significant differences between the conformations assumed by certain proteins in solution and in the solid state makes it imperative that such techniques be developed.[1,2] Otherwise, investigation of the mechanism of action of enzymes and proteins by the integration of functional data obtained from solution studies with structural data derived from X-ray diffraction studies of crystals is difficult or impossible.

As a result of their inherent dependence upon the orientation of the electronic transition dipoles of a molecule, few, if any, spectroscopic techniques are more sensitive to molecular conformation than optical rotatory dispersion (ORD) and circular dichroism (CD). Over the past few years, several investigators have developed theoretical methods which permit the semiquantitative calculation of the chiroptical properties of a molecule as a function of conformation. One such formalism, which is a matrix formulation of the theory of optical activity, has been developed and applied to a diverse array of problems.[3-6] This method is based upon the configuration interaction of excited states, and implicitly includes all of the specialized mechanisms involving the interaction of molecular groups which are known to be of importance in the generation of optical rotatory power.

A preliminary report from this laboratory describing the application of this theoretical method to the calculation of the chiroptical properties of the ^1L_a transitions of the tyrosine residues of ribonuclease S (RNase S) has been published.[7] In addition, Strickland[8] has utilized a different theoretical approach to investigate the optical activity of lower energy transitions which arise from the side-chain chromophores of this protein. The present paper is a report on the application of an origin-independent version of the matrix formalism of Bayley et al.[3] to all of the side-chain chromophoric groups which make significant contributions to the near-UV CD spectrum of RNase S.

The experimental CD spectra of ribonuclease A, S, S′, and S-protein have been reported previously,[9-17] There appears to be a negative near-UV Cotton effect near 275 nm and a positive band of varying intensity near 240 nm. The negative band at 275 nm is thought to arise from some of the six tyrosine residues with possible additional contributions from the four disulfides.[9-14] It has been suggested that the predominant contribution to this band arises from the interaction of tyrosines-73 and -115.[8] The positive band at 240 nm increases in magnitude with increasing pH and decreasing temperature.[10,13] This would suggest that the tyrosine residues that are exposed to the solvent make at least partial contributions to the positive ellipticity of this band. However, disulfide contributions in this region of the spectrum have not been ruled out.[9,18-20]

Experimental Methods

Bovine ribonuclease S, grade XII-S, was purchased from Sigma Chemical Co. and used without further purification. All protein solutions were 0.1 N in sodium chloride. Concentrations of protein were determined spectroscopically by using a molar absorbance of 9800 M^{-1} at 277.5 nm and a molecular weight of 13 683.[21,22] The pH of the sample solutions was adjusted to within 0.1 pH unit by the addition of NaOH or HCl. A 1.0-cm cell was used for recording CD spectra in the wavelength region from 320 to 235 nm and 0.05–0.01-cm cells were used at lower wavelengths.

All CD spectra were recorded on an extensively modified Cary 60 recording spectropolarimeter which utilizes a Princeton Applied Research Model 124A lock-in amplifier for signal detection. The data were acquired with the aid of a PDP-11 digital computer which is equipped with a GT-40 graphics display system. The computer was programmed to average data for a predetermined number of scans, process the data, and display the results on the

† Taken in part from the Ph.D. Dissertation of Warren J. Goux.

(1) B. L. Vallee, J. F. Riordan, J. T. Johansen, and D. M. Livingston, *Cold Spring Harbor Symp. Quant. Biol.*, **36**, 517 (1972).
(2) J. Moult, A. Yonath, W. Traub, A. Similansky, A. Podjorny, D. Rabiknovich, and A. Saya, *J. Mol. Biol.*, **1**, 179–195 (1976).
(3) P. M. Bayley, E. B. Nielsen, and J. A. Schellman, *J. Phys. Chem.*, **73**, 228–243 (1969).
(4) T. M. Hooker, Jr., and J. A. Schellman, *Biopolymers*, **9**, 1319–1348 (1970).
(5) V. Madison and J. A. Schellman, *Biopolymers*, **11**, 1041–1076 (1972).
(6) T. M. Hooker, Jr., P. M. Bayley, W. Radding, and J. A. Schellman, *Biopolymers*, **13**, 549–566 (1974).
(7) W. J. Goux and T. M. Hooker, Jr., *J. Am. Chem. Soc.*, **97**, 1605–1606 (1975).
(8) E. H. Strickland, *Biochemistry*, **11**, 3465–3474 (1972).
(9) J. Horwitz, E. H. Strickland, and C. Billups, *J. Am. Chem. Soc.*, **92**, 2119–2129 (1970).
(10) M. N. Pflumm and S. Beychock, *J. Biol. Chem.*, **244**, 3973–3981 (1969).
(11) M. N. Pflumm and S. Beychock, *J. Biol. Chem.*, **244**, 218–221 (1969).
(12) E. R. Simons and E. R. Blout, *J. Biol. Chem.*, **243**, 218–221 (1967).
(13) E. R. Simons, E. G. Schneider, and E. R. Blout, *J. Biol. Chem.*, **244**, 4023–4026 (1969).
(14) R. T. Simpson and B. L. Vallee, *Biochemistry*, **5**, 2531–2538 (1966).
(15) J. A. Schellman and M. J. Lowe, *J. Am. Chem. Soc.*, **90**, 1070–1072 (1968).
(16) C. B. Anfinsen and E. Haber, *J. Biol. Chem.*, **236**, 1361–1363 (1961).
(17) S. Beychock, *Proc. Natl. Acad. Sci. U.S.A.*, **53**, 999–1006 (1965).
(18) S. Beychock, *Science (Washington, D.C.)*, **154**, 1288–1299 (1966).
(19) E. Breslow, *Proc. Natl. Acad. Sci. U.S.A.*, **67**, 493–500 (1970).
(20) S. Beychock and E. Breslow, *J. Biol. Chem.*, **243**, 151–156 (1968).
(21) M. Sela and C. B. Anfinsen, *Biochim. Biophys. Acta*, **24**, 229–235 (1957).
(22) C. H. W. Hirs, S. Moore, and W. H. Stein, *J. Biol. Chem.*, **235**, 633–647 (1960).

0002-7863/80/1502-7080$01.00/0

graphics display unit and an associated terminal. It is possible to measure CD difference spectra with this instrumentation by repetitively scanning the spectra of interest, storing the data on magnetic disks, then subtracting one spectrum from the other by means of computer software. All spectra were scanned at rates of from 35 to 70 nm/min with appropriate time constants. Details of this instrumentation will be described in a future publication.

Theoretical Methods

The theoretical formalism which was employed to calculate the chiroptical properties of RNase S is similar to that used previously for the investigation of several model compounds.[2,23-26] The present method is an origin-independent variant of the matrix formalism of Bayley et al.,[3] which is based upon ideas first suggested by John Schellman in 1968. Instead of calculating rotatory strengths by means of electric and magnetic transition dipole moments and eq 1, transition linear and angular momenta are

$$R_{0K} = \text{Im}\,\{\mu_{0K}\cdot\mathbf{M}_{K0}\} \tag{1}$$

utilized to define a quantity, the chiral strength, c_{0K}, which is the chiroptical analogue of the oscillator strength of ordinary spectroscopy. The chiral strength, one of several known moments of the rotatory strength,[27,28] is defined by eq 2 where α is the fine

$$c_{0K} = \frac{\alpha}{3}\,\text{Re}\,\{\mathbf{p}_{0K}\cdot\mathbf{L}_{K0}\} \tag{2}$$

structure constant, $\mathbf{p}_{0K}$ is the linear momentum moment, $\mathbf{L}_{K0}$ is the angular momentum moment, and all quantities are expressed in atomic units. This formalism avoids the origin dependence and conservation problems associated with the calculation of rotatory strengths with finite basis sets by means of the original matrix method.[3,29,30] Transition linear and angular momenta can be determined from known electric and magnetic transition moments. Theoretical chiral strengths can be readily compared with experimental circular dichroism spectra by calculating molar ellipticities by means of eq 3, where λ_{0K} is the characteristic

$$M_\theta = \frac{18Ne^2}{\sqrt{\pi}mc^2}\,\frac{\lambda_{0K}{}^2}{\Delta_{0K}}\,e^{-[(\lambda-\lambda_{0K})/\Delta_{0K}]^2}c_{0K} \tag{3}$$

wavelength in cm (a factor of 10^{-7} must be included in eq 3 if wavelengths are expressed in nm), Δ_{0K} is the exponential half-width, and the other symbols have their usual meanings. The numerical value of the constant term at the beginning of the equation is 1.7234×10^{12}. Furthermore, chiral strengths can be converted to rotatory strengths by eq 4.

$$R_\theta = \frac{3he^2}{8\pi^2mc}\lambda_{0K}c_{0K} \tag{4}$$

The procedure for carrying out actual calculations is essentially the same as that reported by Bayley et al.[3] That is, an interaction Hamiltonian matrix is set up and transformed to diagonal form by a unitary matrix, yielding the eigenvalues and eigenvectors for the problem. The unitary matrix is used to transform linear and angular momentum moments from the independent systems representation into the interaction representation. These moments are then used in eq 2 to compute chiral strengths. In the present case, eq 4 has been employed to convert the calculated chiral strengths to the more familiar rotatory strengths.

In order to utilize side-chain chromophores as probes of local structure, it is necessary to assess the contributions which transitions localized on specific chromophores make to the strength of a given CD band. To a first approximation, one can consider the sign and magnitude of the chiral strength that arises from the mutual interaction of two electronic transitions to be dependent upon the product of two terms, the interaction energy and the optical factor.[31] The interaction energy is the energy associated with the electrostatic interaction between the transitions which are coupling whereas the optical factor depends upon the relative geometries of the transition moments. Thus, a given transition may give rise to a large Cotton effect as a result of a large interaction energy, a large optical factor, or both. Since the magnitude of the interaction energy will vary inversely with distance, a pair of transitions may not give rise to a significant contribution to the chiroptical power if they are too widely separated. On the other hand, even though two transitions are in close proximity, they may not couple significantly unless the optical factors are favorable.

In the present theoretical formalism, there is extensive mixing of many of the localized transitions to produce final eigenstates of the system. This is especially true for transitions which are degenerate or near degenerate with other transitions in the protein, e.g., the ^1L_b excited states of the six tyrosine residues.[7,8] Since extensive mixing of excited states can occur, one cannot always correlate specific electronic transitions localized on given amino acid residues with observed spectral features. Indeed, in theory, the chiral strength of a given transition is influenced to some extent by all of the transitions on the remaining chromophoric groups of the molecule. However, since the chiral strength that is developed by a given transition, or group of transitions, depends upon the energies, physical separation, and orientation of the transition moments, certain interactions should be more significant than others. It is possible to estimate the relative significance of coupling interactions by careful analysis of the eigenvectors and the individual intertransition coupling terms which are summed to determine the overall chiral strength of the band under consideration. This is not a trivial undertaking in the case of a problem such as the present one since it is necessary to investigate the elements of N arrays of dimension $N \times N$, where N is the number of electronic transitions in the basis set. Nevertheless, in many cases, it is possible to at least estimate the contribution of some specific interchromophore interactions to certain spectral features.

The spectroscopic data needed for the calculation include energies and polarizations for the electronic transitions on each chromophore. Data for the peptide chromophore were taken from the paper by Bayley, Nielsen, and Schellman[3] except for the fact that a wavelength of 220 nm was utilized for the amide $n-\pi^*$ transition instead of 212 nm.[32] Tyrosine optical parameters were calculated from the data used in previous model-compound investigations.[4] Although optical data for histidine are available both for the protonated and free-base forms,[23] calculations have been carried out for only the protonated form. No attempt was made to include the electronic transitions of phenylalanine, since these transitions apparently make only minor contributions to the near-UV CD spectra.

Ribonuclease has four disulfide bridges formed by cystines-26–84, -40–95, -58–110, and -65–72.[33] Transitions on these chromophores may give rise to optical activity in the near-UV by interaction with transitions occurring on other groups in the molecule. An additional contribution can arise from inherent dissymmetry of the disulfide group. If one considers only the data taken from the 7B set of coordinates, which is a set which has been refined to fit X-ray intensities, the only disulfide in RNase S which might be expected to give rise to a really large chiral

(23) P. E. Grebow and T. M. Hooker, Jr., *Biopolymers*, **14**, 871–881 (1975).
(24) J. W. Snow and T. M. Hooker, Jr., *J. Am. Chem. Soc.*, **96**, 7800–7806 (1974).
(25) W. J. Goux, T. R. Kadesch, and T. M. Hooker, Jr., *Biopolymers*, **15**, 977–997 (1976).
(26) J. W. Snow and T. M. Hooker, Jr., *J. Am. Chem. Soc.*, **97**, 3505–3511 (1975).
(27) A. Hansen, *Mol. Phys.*, **33**, 483–494 (1977).
(28) D. Caldwell, *Mol. Phys.*, **33**, 495–510 (1977).
(29) S. Chandrasekhar, *Astrophys. J.*, **102**, 223–231 (1945).
(30) A. Moscowitz, Ph.D. Thesis, Harvard University (1957); in "Modern Quantum Chemistry", O. Sinanoglu, Ed., Academic Press, New York, 1965, pp 31–44.
(31) J. A. Schellman, *Acc. Chem. Res.*, **1**, 144–151 (1968).
(32) R. W. Woody, *J. Chem. Phys.*, **49**, 4797–4806 (1968).
(33) F. M. Richards and H. W. Wyckoff, *Enzymes*, *3rd Ed. 4*, 647, (1971).

strength by virtue of its inherent dissymmetry is cystine-40–95, as the others have dihedral angles that are reasonably near 90°. Since the 7B coordinates were utilized for these calculations, inherent dissymmetry contributions to the chiral strength arise only from cystine-40–95. However, it should be pointed out that disulfide dihedral angles determined from some earlier sets of coordinates indicate appreciable deviations from 90° for several of the residues.

Linderberg and Michl[34] were the first to extend the model proposed by Bergson[35,36] to the calculation of transition energies and the inherent optical activity of the disulfide chromophore. Woody[37] has recently extended the Bergson treatment of the disulfide group to include two additional transitions. His theory suggests these two transitions arise from excitation of nonbonding orbitals, predominantly 3s in nature, to σ excited states. These transitions, which he designates as $n_2-\sigma^*$ and $n_3-\sigma^*$, are degenerate for dihedral angles of ±90°. Woody also predicts two other $n-\sigma^*$ transitions which arise from nonbonding orbitals that are predominantly 3p in nature. These transitions have properties similar to the $n-\sigma^*$ transitions of Linderberg and Michl, and are designated $n_1-\sigma^*$ and $n_4-\sigma^*$. At dihedral angles of ±90°, the $n_1-\sigma^*$ and $n_4-\sigma^*$ transitions are also degenerate. Optical data, including the electric and magnetic transition dipole moments associated with the four $n-\sigma^*$ transitions, are presented by Woody. These optical parameters have been adapted for inclusion in the present calculations. Although these data may represent an oversimplification, they have been successfully used for the calculation of the chiroptical properties of the epidithiopiperazinedione group.[38]

An additional problem arises in assigning energies to the four disulfide transitions. Woody's theory predicts that all four $n-\sigma^*$ transitions should occur in the UV region above 190 nm. Transitions from the π-type n_1 and n_4 nonbonding orbitals should lie lower in energy than the σ-type n_2 and n_3 orbitals. The SCF calculations of Yamabe et al.,[39] in which contributions from 3d and 4s orbitals were neglected, preserve this simplified picture of π-type and σ-type nonbonding orbitals. For dihedral angles of ±90°, this work predicts that the two σ-type nonbonding orbitals lie 1–2 eV lower in energy than the two π-type orbitals. However, some theoretical calculations in which 3d orbitals are included indicate that the situation may be somewhat more complicated. For example, CNDO calculations carried out by Richardson et al.[40] predict that for a dihedral angle of 90° there should be six disulfide transitions, all to the red of 230 nm.

Numerous experimental studies on sterically constrained disulfide systems of known chirality have also been undertaken.[41-48] Absorption and CD studies on 1,2-dithianes indicate that the variation in energy of the long-wavelength $n-\sigma^*$ transitions with change in dihedral angle agrees reasonably well with the predictions of the Bergson model.[43] The σ-type $n-\sigma^*$ transitions are not as well understood but are thought to occur in the 190–205-nm region of the spectrum. As might be expected from simple molecular orbital theory, these higher energy transitions appear to be less sensitive to changes in dihedral angle.

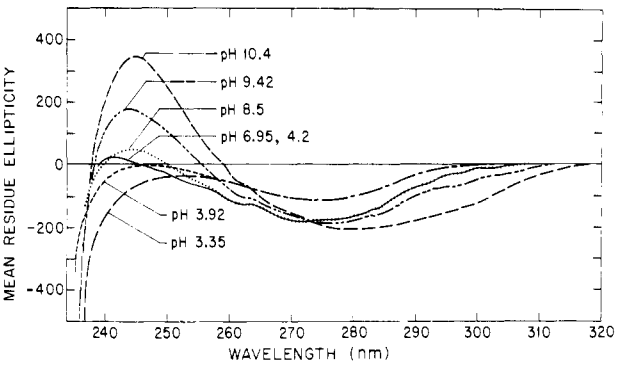

Figure 1. Near-ultraviolet circular dichroism spectra of ribonuclease S as a function of pH. All curves represent an average of four sample scans and four base-line scans. Ionic strength was 0.1, and the temperature was 27 °C for all solutions.

Wavelengths of 250 nm were assigned to the $n_1-\sigma^*$ and $n_4-\sigma^*$ transitions for those disulfides which have dihedral angles near ±90°. This is in reasonable agreement with the assignment of these transitions at 250 nm in the vapor-phase spectrum of dimethyl disulfide and at 252–256 nm in L-cystine derivatives.[49,50] However, the situation is somewhat more complicated in the case of the disulfide which has a dihedral angle of −70°. In this case, the $n_1-\sigma^*$ and $n_4-\sigma^*$ bands should be split, one to the red of 250 nm and the other to the blue. For example, difference CD spectra of 2,7-bis[*S*-(acetamidomethyl)cysteine]gramicidin S, which has a disulfide dihedral angle of 120°, reveal bands at 272 and 230 nm.[48] Thus, in the present calculations, the $n_1-\sigma^*$ and $n_4-\sigma^*$ transitions of cystine-40–95 were assigned at 260 and 240 nm, respectively.

There is even more uncertainty in the wavelength of the higher energy disulfide transitions.[37,49,50] In any event, these transitions are less likely to couple strongly with the near-UV transitions which are of interest in this investigation. Since the omission of these transitions from the calculation should not lead to serious errors insofar as the interpretation of the chiroptical properties of the near-UV chromophores are concerned, they have not been included.

RNase S coordinates were supplied by Wyckoff and Powers of Yale University. Hydrogen atoms were added to the α carbon and amide nitrogen atoms, assuming standard bond angles and distances.[51] Static charges were obtained for each of the amino acid residues by using the method of Del Re, Pullman, and coworkers[52] as presented by Poland and Scheraga.[53]

Theoretical calculations initially carried out on polypeptide model systems have indicated that if effects due to highly ordered secondary structure are of no concern most of the optical activity of a protein can be accounted for by including only the structure in the immediate vicinity of the chromophores of interest. Since it is the primary objective of the present study to account for the near-UV optical activity originating from side-chain chromophores, the only amide transitions included in the calculations were those which fell within 8 Å of the γ carbon of each tyrosine side chain and the amides immediately adjoining each of the cystine residues.

An effective dielectric constant of two has been assumed for all computations. The calculations were carried out on the Itel AS-6 computer of the University of California, Santa Barbara Computer Center.

(34) J. Linderberg and J. Michl, *J. Am. Chem. Soc.*, **92**, 2619–2625 (1970).
(35) G. Bergson, *Ark. Kemi*, **12**, 233–237 (1958); **18**, 409–434 (1962).
(36) G. Bergson, G. Claeson, and L. Schotte, *Acta Chem. Scand.*, **16**, 1159–1165 (1962).
(37) R. W. Woody, *Tetrahedron*, **29**, 1273–1283 (1973).
(38) R. Nagarajan and R. W. Woody, *J. Am. Chem. Soc.*, **95**, 7212–7222 (1973).
(39) H. Yamabe, H. Kato, and T. Yonezawa, *Bull. Chem. Soc. Jpn.*, **44**, 604–610 (1971).
(40) R. W. Strickland, J. Webb, and F. S. Richardson, *Biopolymers*, **13**, 1269–1290 (1974).
(41) N. Ito and T. Takagi, *Biochim. Biophys. Acta*, **221**, 430–441 (1970).
(42) A. Imanishi and T. Isemura, *J. Biochem. (Tokyo)*, **65**, 309–312 (1969).
(43) M. Carmack and L. A. Neubert, *J. Am. Chem. Soc.*, **96**, 943–945 (1974).
(44) M. Carmack and L. A. Neubert, *J. Am. Chem. Soc.*, **89**, 7134–7136 (1967).
(45) R. M. Dodson and V. C. Nelson, *J. Org. Chem.* **33**, 3966–3968 (1968).
(46) G. Claeson, *Acta Chem. Scand.*, **22**, 2429–2436 (1968).
(47) B. Donzel, B. Kamber, K. Wuthrich, and R. Schwyzer, *Helv. Chim. Acta*, **55**, 947–961 (1972).
(48) U. Ludescher and R. Schwyzer, *Helv. Chim. Acta*, **54**, 1637–1644 (1971).
(49) D. L. Coleman and E. R. Blout, *J. Am. Chem. Soc.*, **90**, 2405–2415 (1968).
(50) S. D. Thompson, D. G. Carroll, F. Watson, M. O'Donnell, and S. P. McGlynn, *J. Chem. Phys.*, **45**, 1367–1379 (1966).
(51) L. Pauling, "Nature of the Chemical Bond", 3rd ed., Cornell University Press, Ithaca, NY, 1960.
(52) G. Del Re, *J. Chem. Soc.*, 4031–4040 (1958); G. Del Re, B. Pullman, and T. Yonezawa, *Biochim. Biophys. Acta*, **75**, 153–182 (1963).
(53) D. Poland and H. A. Scheraga, *Biopolymers*, **6**, 3791–3800 (1967).

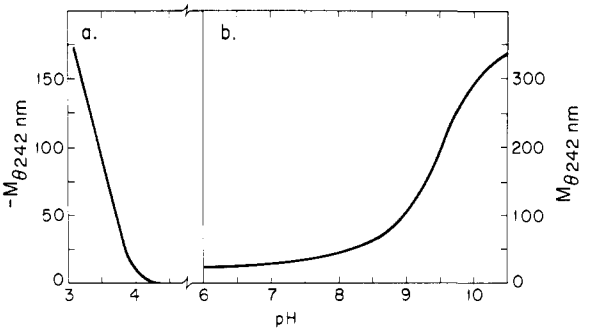

Figure 2. Mean-residue ellipticity of ribonuclease S at 242 nm as a function of pH.

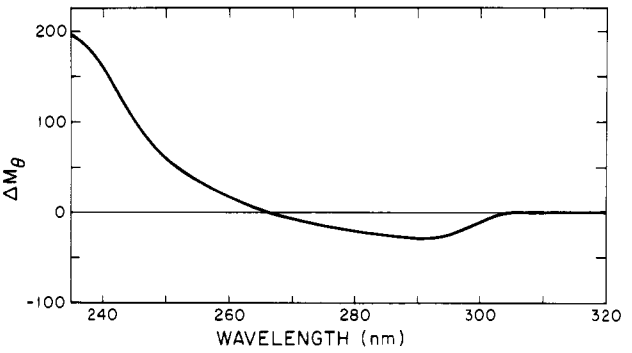

Figure 3. Circular dichroism difference spectrum of ribonuclease S in the presence of 3′-cytosine monophosphate vs. ribonuclease S (ribonuclease S with 3′-cytosine monophosphate–ribonuclease S). Ionic strength 0.1; temperature 27 °C. Curve is an average of four scans.

Experimental Results

Figure 1 shows near-UV CD spectra of RNase S in dilute salt solution as a function of pH. At all pH values investigated, there is a negative Cotton effect near 275 nm. Between pHs 4.2 and 8.5, there are no marked changes in the ellipticity of the 275-nm band. Fine structure associated with the band is visible at 261 and 283 nm. Strickland et al.[9] have reported similar fine structure in the low-temperature CD spectra of ribonuclease A. At pH 3.35, the band is decreased in amplitude by roughly 50%. In more acidic solutions, the magnitude of the band is decreased even more. However, these changes are reversible, as can readily be demonstrated by neutralization of the acidic solutions. These results are consistent with other data for the reversible denaturation of RNase in acidic solutions.[33,54-56] At pH values above 8.5, the 275-nm band increases in magnitude and is shifted to the red. Similar CD data have been reported for RNase A.[10,11]

There is a small positive Cotton effect at 241 nm at pH values from 4.2 to 6.95. A magnitude of 25 deg cm^2/dmol was observed at the extremum of this band. This is somewhat lower than the value reported by Pflumm and Beychock under slightly different conditions.[10,11] Under more alkaline conditions, the band increases markedly in intensity and shifts to the red. Similar behavior has been reported previously by others.[12,13]

The ellipticity of the 240-nm band at the extremum is plotted as a function of pH in Figure 2. A derivative plot of these data yields an apparent pK of 9.5. Although this value must be regarded as only an approximate one, it is in reasonable agreement with the intrinsic pK of 9.66 which has been reported for the exposed tyrosine residues of RNase A by Tanford and co-workers.[57] As the pH is decreased below 4.0, the band at 241 nm decreases in magnitude and is blue shifted. It was not possible to observe a low pH plateau in the titration curve. However, the low pH portion of the curve shown in Figure 2 is in agreement with the spectroscopic titration of RNase S as reported by Richards and Logue.[55]

In order to determine the effect of binding inhibitors, the CD difference spectra of RNase S and RNase S in the presence of 3′-cytosine monophosphate (3′-CMP) were measured over the wavelength region of interest. The results of these investigations are presented in Figure 3. The difference spectrum reveals an increase in the magnitude of both the negative Cotton effect at 275 nm and the positive one in the 240-nm region upon binding of 3′-CMP.

Theoretical Results

Results of the calculation of the chiroptical properties of the near-UV absorbing side-chain transitions of RNase S are reported in Table I. Calculated rotatory strengths and wavelengths are presented for the tyrosine, cystine, and histidine residues. Data are shown for the two lowest energy disulfide transitions, i.e., the ones which are designated as the n_1–σ^* and n_4–σ^* transitions by Woody.[37] Where appropriate, the rotatory strengths which are reported include contributions that arise from inherent dissymmetry. Results are also given for the four lowest energy transitions that are associated with the phenolic chromophore of tyrosine and the two lowest energy imidazole transitions. The imidazole transitions are denoted as I_1 and I_2 for the higher and lower wavelength bands, respectively, whereas the Platt notation[58,59] is employed for the phenolic bands.

Table I. Theoretical Mean Residue Rotatory Strengths for Selected Side-Chain Transitions of Ribonuclease S

residue	transition	wavelength, nm	R (DBM)
Tyr-25	^1L_b	275.1	0.00338
	^1L_a	225.9	0.00488
	^1B_b	195.0	0.0669
	^1B_a	192.6	0.00381
Tyr-73	^1L_b	275.1	0.00217
	^1L_a	225.7	0.00266
	^1B_b	197.5	−0.0290
	^1B_a	195.3	−0.171
Tyr-76	^1L_b	275.0	−0.00633
	^1L_a	225.1	0.0591
	^1B_b	194.9	0.106
	^1B_a	193.6	−0.00414
Tyr-92	^1L_b	275.1	−0.00143
	^1L_a	225.2	0.353
	^1B_b	196.6	−0.0359
	^1B_a	193.5	0.0213
Tyr-97	^1L_b	275.0	0.00317
	^1L_a	225.1	−0.0689
	^1B_b	195.7	−0.00991
	^1B_a	194.5	−0.0328
Tyr-115	^1L_b	275.0	−0.00106
	^1L_a	224.7	−0.0179
	^1B_b	192.2	−0.124
	^1B_a	194.7	0.166
Cys-26–Cys-84	n_1–σ^*	250.2	−0.00101
	n_4–σ^*	250.1	0.00509
Cys-40–Cys-95	n_1–σ^*	260.2	−0.00381
	n_4–σ^*	240.1	0.0101
Cys-58–Cys-110	n_1–σ^*	250.2	0.00443
	n_4–σ^*	250.2	0.000324
Cys-65–Cys-72	n_1–σ^*	250.1	−0.00358
	n_4–σ^*	250.4	−0.00315
His-12	I_1	207.0	−0.0850
	I_2	179.2	−0.00537
His-48	I_1	207.2	0.0759
	I_2	179.4	0.00461
His-105	I_1	206.6	−0.00186
	I_2	179.7	0.00191
His-119	I_1	205.1	0.0172
	I_2	179.8	−0.000633

(54) H. B. Bull and K. Breese, *Arch. Biochem. Biophys.*, **117**, 106–109 (1966).
(55) F. M. Richards and A. D. Logue, *J. Biol. Chem.*, **237**, 3693–3697 (1962).
(56) C. Tanford and J. A. Hauenstein, *J. Am. Chem. Soc.*, **78**, 5287–5291 (1956).
(57) C. Tanford, J. D. Hauenstein, and D. G. Rands, *J. Am. Chem. Soc.*, **77**, 6409–6413 (1955).
(58) J. R. Platt, *J. Chem. Phys.*, **17**, 484–495 (1949).
(59) J. R. Platt, *J. Opt. Soc. Am.*, **43**, 252–257 (1953).

Table II. Principal Coupling Interactions Contributing to the Rotatory Strength of Tyrosine Residues (^1L_b and ^1L_a Transitions)[a]

	Tyr-25		Tyr-73		Tyr-76		Tyr-92		Tyr-97		Tyr-115	
	^1L_b	^1L_a	^1L_b	^1L_a	^1L_b	^1L_a	^1L_b	^1L_a	^1L_b	^1L_a	^1L_b	^1L_a
Asn-24 π-π^*		−−		++						−−		−
Tyr-25 ^1B_b							−					
Tyr-25 ^1B_a				++						−−		
Tyr-25 n-π^*		+++										
Tyr-25 π-π^*	++	++		+	++		−		−			
Cys-26-Cys-84 n_1-σ^*	−−						+		+			
Cys-26-Cys-84 n_4-σ^*	−−								+			
Cys-26 π-π^*	−	++			−							
Asn-27 π-π^*									+			
Gln-28 π-π^*		−−										
Thr-36 π-π^*	+				+							
Lys-37 π-π^*	−	++				−−−	+	−−−	−	−−		
Asp-38 π-π^*								−−−	−	−		
Arg-39 π-π^*						−−						
Cys-40-Cys-95 n_1-σ^*	−				−		+		−			
Cys-40-Cys-95 n_4-σ^*							+		+	++		
Lys-41 n-π^*										++		
Lys-41 π-π^*		++	+			−−	+	+			−	
His-48 I_1	−	+++		++			−	++		−−		−−
Ala-56 π-π^*			−	++							+	++
Cys-58-Cys-110 n_4-σ^*			+		+						+	
Cys-58 n-π^*				−−								++
Gln-60 n-π^*						++						
Gln-60 π-π^*	−		+		+	−−		−−		−−−	+	
Lys-61 π-π^*			−								+	
Thr-70 π-π^*			−	++	−						−	
Asn-71 n-π^*				−−								−−
Asn-71 π-π^*				−−								−−
Cys-72 π-π^*			−	+++	−	++					+	+
Tyr-73 ^1L_a					+						−	
Tyr-73 ^1B_b		−−						−−			+	−−−
Tyr-73 ^1B_a		++			+				−		−−	+++
Tyr-73 π-π^*											+	−−
Gln-74 π-π^*			−		−						−	++
Ser-75 π-π^*		++				+++		++				
Tyr-76 ^1B_a								++				
Asp-83 π-π^*					+							
Cys-84 π-π^*								−−				
Arg-85 π-π^*	+				−		−	++	−			
Glu-86 π-π^*								−		++		
Tyr-92 ^1B_b	−								+			
Tyr-92 ^1B_a						−−				++		
Tyr-92 n-π^*								++				
Tyr-92 π-π^*						−−	−			++		
Pro-93 π-π^*						−−				−−		
Asn-94 π-π^*	−						+					
Cys-95 π-π^*	+		−				−		+		+	
Ala-96 π-π^*						++	−	−	−	+++	+	
Tyr-97 ^1B_b		+++					+					
Tyr-97 ^1B_a		−−−			+			++				++
Tyr-97 π-π^*					−			−				
Lys-98 π-π^*		−−					−	++				
His-105 I_1						−−						
Val-108 π-π^*										++		
Ala-109 π-π^*											+	
Cys-110 n-π^*				+								+++
Cys-110 π-π^*				−−		++						
Glu-111 π-π^*			+		−						−	
Gly-112 π-π^*			−									
Pro-114 π-π^*				−−								
Tyr-115 ^1L_a			−−									
Tyr-115 ^1B_b			+	−−−								
Tyr-115 ^1B_a		+	−−	+++	+	++	−					
Tyr-115 π-π^*		−−										
Pro-117 π-π^*				−−								
His-119 I_1				−−								

[a] See text for definition of symbols.

As was pointed out earlier, it is possible to estimate the relative significance of various intertransition interactions in the origin-independent matrix formalism. Tables II and III summarize rotatory strength contributions associated with the tyrosine ^1L_b and ^1L_a transitions, and the disulfide n-σ^* transitions, which result from coupling interactions; contributions which arise from inherent dissymmetry are not included. The symbols represent weak, moderately strong, and very strong positive or negative contributions to the rotatory strengths of the transitions listed across the top of each table. Three plus or minus symbols indicate that the approximate contribution to the rotatory strength is greater than or equal to 10^{-3} DBM, two symbols denote a magnitude

Table III. Principal Coupling Interactions Contributing to the Rotatory Strength of Cystine n_1-σ^* and n_4-σ^* Transitions[a]

	Cys-26-84		Cys-40-95		Cys-58-110		Cys-65-72	
	n_1-σ^*	n_4-σ^*	n_1-σ^*	n_4-σ^*	n_1-σ^*	n_4-σ^*	n_1-σ^*	n_4-σ^*
Asn-24 π-π^*		−−						
Tyr-25 ^1B_b	−−	−−			++	+	+++	
Tyr-25 π-π^*	−−							
Asn-27 π-π^*	−	++						
Gln-28 π-π^*		++						
Met-29 π-π^*	−−							
His-48 I_1		++						
Ala-56 π-π^*						−−		++
Thr-36 π-π^*			−					
Asn-38 π-π^*			−	+				
Val-57 π-π^*					−−			−−
Cys-58 π-π^*	++	−−						
Val-63 π-π^*							−−	−−
Cys-65 π-π^*					−	−	−	−−
Thr-70 π-π^*						−	++	−
Asn-71 π-π^*					++	−−	++	++
Cys-72 π-π^*						−−		++
Tyr-73 ^1L_a					++	+	+	−−
Tyr-73 ^1L_b	++				−−	++	++	++
Tyr-73 ^1B_a	++				+++	−−	+	+
Thr-82 π-π^*	++	+						
Asp-83 π-π^*		−−						−
Ser-90 π-π^*				−				
Lys-91 π-π^*			+	+				
Tyr-92 ^1L_a				+				
Tyr-92 ^1B_b			+	+				
Tyr-92 ^1B_a				+				
Pro-93 π-π^*			+					
Asn-94 π-π^*			−					
Ala-96 π-π^*	+							
Tyr-97 ^1L_a	+	++	+	++				
Tyr-97 ^1B_b	++	++		+				
Tyr-97 ^1B_a	++	+++	+	++	+	++	−	+
Lys-98 π-π^*	++	−−				−−		
Thr-99 π-π^*	++	−−						
Thr-100 π-π^*		++						
Val-108 π-π^*					++		++	++
Ala-109 π-π^*						−−	−−	++
Tyr-115 ^1B_b	+	+			++	++	−−	++
Tyr-115 ^1B_a		++			++		++	
Tyr-115 π-π^*					++	−−	−	+
Val-116 π-π^*		+			++	−−−		++
His-119 I_1						−−	++	−−−

[a] See text for definition of symbols.

which is less than 10^{-3} but greater than or equal to 10^{-4} DBM, and one symbol indicates that the contribution is less than 10^{-4} but greater than 10^{-5} DBM. For example, the π-π^* transition of the peptide group of tyrosine-25 interacts with the ^1L_a transition of the phenolic chromophore of the same residue to make an estimated contribution of between 10^{-4} and 10^{-3} DBM to the rotatory strength near 225 nm.

As was pointed out earlier, since there is extensive mixing of the degenerate transitions after configuration interaction, it is often impossible to assign a rotatory strength contribution to a single residue. Thus, the π-π^* transition of the lysine-37 peptide interacts strongly with the ^1L_a transitions of tyrosines-25, -76, -92, and -97 to make a net negative contribution to the rotatory strength of the ^1L_a bands. The coupling of the ^1L_b, ^1L_a, and ^1B_a transitions of specific tyrosine residues with the ^1L_b excited-state configurations of other tyrosine residues gives rise to a net negative contribution to the rotatory strength near 275 nm. A large positive rotatory strength contribution is associated with the tyrosine ^1L_a bands as a result of extensive coupling with the ^1B_b and ^1B_a transitions of other residues.

A quantitative summary of the results of two different sets of calculations of the rotatory strengths of the near-UV absorbing chromophores of RNase S is shown in Table IV. The data in the first column of the table were obtained from calculations in

Table IV. Summary of Calculated Mean Residue Rotatory Strengths for Ribonuclease S

transition	Tyr, His, and 8-Å peptides	Tyr, His, Cys, and 8-Å peptides
Tyr ^1L_b	−0.0026	−0.0001
Tyr ^1L_a	0.020	0.0079
Cys n-σ^* (260 nm)		−0.0038
Cys n-σ^* (250 nm)		0.0021
Cys n-σ^* (240 nm)		0.010

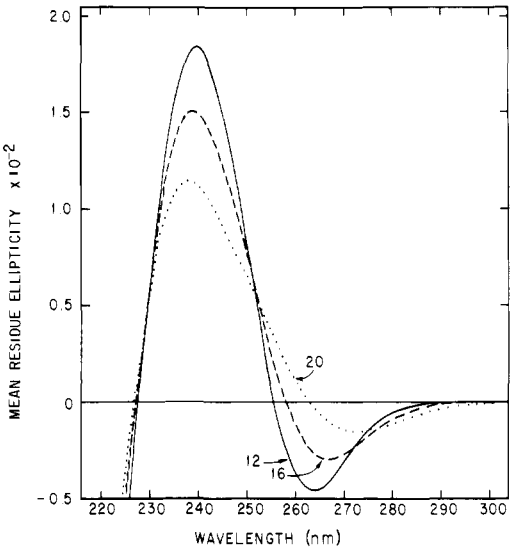

Figure 4. Theoretical circular dichroism spectra of ribonuclease S. Gaussian band shapes assumed. All bandwidths were 12 nm except for the disulfides which were as indicated on the figure.

which only the six tyrosine residues, the histidines, their adjacent amide groups, and all additional amide chromophores within 8 Å were included in the basis set. The data in the second column were obtained with a basis set which included all of the above chromophores plus the four disulfide chromophores of the cystine residues. These data include the rotatory strength contribution due to disulfide inherent dissymmetry. Calculated CD spectra are shown in Figure 4. All of the curves were computed from theoretical results which included the disulfide chromophores, and resulting inherent contributions to the rotatory strength. The curves differ only in that different bandwidths, i.e., half-widths at $1/e$ of maximum amplitude, were used for the disulfide transitions; values of 12, 16, and 20 nm were employed. Bandwidths of 12 nm were utilized for all other transitions.

Discussion

The data of Table II suggest that many of the peptide transitions surrounding the tyrosine side-chains couple with the ^1L_b transitions. However, for the most part, it appears that these interactions make only relatively small contributions to the rotatory strength of the ^1L_b states.

The only disulfide transitions which make appreciable contributions to the rotatory strength of the tyrosine ^1L_b bands are the n_1-σ^* and n_4-σ^* transitions of cystines-26–84 and -40–95, and the n_4-σ^* transition of cystine-58–110. These transitions interact predominantly with tyrosines-25, -92, and -97. Presumably, this is a result of large interaction energy terms resulting from the proximity of these disulfides to the tyrosine residues involved.

The predominant contributions to the rotatory strength of the tyrosine ^1L_b bands arise from coupling interactions among the tyrosines themselves. Especially noteworthy is the interaction between tyrosines-73 and -115. Coupling of the ^1B_a transitions on residues 73 and 115 and the ^1L_b states of tyrosines-115 and -73, respectively, gives rise to a large portion of the rotatory strength associated with the ^1L_b band as summarized in Table II. The close contacts which these residues make with each other,

as well as favorable optical factors, account for this contribution.

At least in principle, one might expect exciton-type interactions to occur among the ^1L_b transitions. Although such interactions should not change the net rotatory strength of a given band, the resulting splitting could drastically alter the band shape, and thereby affect the observed CD spectrum. The formalism which was utilized to carry out these calculations does allow for such interactions, and is capable of computing both the rotatory strength and splitting that might result. However, such degenerate coupling appears to be very small in the case of the tyrosine ^1L_b transitions.

It should be pointed out that many of the coupling interactions which have been found to be important in generating tyrosine ^1L_b rotatory strength were also identified as being significant by Strickland.[8] Most of the differences which do exist are of a quantitative nature, i.e., there is agreement insofar as the sign of the contribution is concerned, but there are differences as to the relative magnitude of the interaction. This is certainly not surprising in view of the fact that the present calculations have been carried out by means of a matrix-based configuration interaction formalism, whereas Strickland's earlier work was based on pairwise coupling. These differences in method certainly might be expected to lead to the assignment of optical activity to somewhat different sources.

The contribution of the tyrosine ^1L_b transitions to the 275-nm CD band is complicated by the possibility of rotation about the dihedral angle χ^2. Semiempirical conformational energy calculations[60] were carried out in an attempt to assess the relative significance of this possibility. These calculations revealed minima in conformational energy which are consistent with the values of χ^2 calculated from the 7B set of X-ray coordinates for all of the tyrosine residues except number 76. In the case of tyrosine-76, conformational energy minima were found near 30, 100, and 140°; the last value essentially coincides with that found in the crystal structure. The minimum at 30° appears to be slightly lower in energy than the minimum at 140° whereas the 100° minimum is slightly higher in energy. A barrier height of less than 1 kcal/mol was calculated, which would indicate that there is a possibility of a significant distribution of conformers at room temperature.

Optical calculations were carried out with χ^2 of tyrosine-76 fixed at these three values. These calculations indicated that more negative rotatory strengths are predicted for the 275-nm Cotton effect when χ^2 of tyrosine-76 assumes values smaller than those found in the crystal. For example, the rotatory strength for the conformer with χ^2 equal to 30° is approximately twofold larger than that calculated for the conformer found in the crystalline state. The increase in negative ellipticity which would result from assuming a value near 30° for χ^2 of tyrosine-76 would bring the theoretical results into better agreement with experiment. However, these results must be considered preliminary since there is considerable uncertainty as to the reliability of semiempirical conformational energy calculations such as these.

As is obvious from Table II, interactions with peptide transitions make a greater contribution to the rotatory strength of the tyrosine ^1L_a bands than was the case for the tyrosine ^1L_b bands. Most of the larger contributions come from coupling with adjoining amide π–π^* transitions. However, significant interactions also occur with peptide n–π^* transitions which lie in the vicinity of the tyrosine side chains. For example, in the case of tyrosine-25, coupling with the n–π^* transition of the adjoining amide group makes a larger contribution to the ^1L_a rotatory strength than the π–π^* transition of the same peptide group does. These interactions appear to result from the μ–m coupling mechanism, which is known to make important contributions in some cyclic peptide systems.[6] However, this mechanism can make significant contributions to the rotatory strength only if the interacting transitions are physically close together.[31] Furthermore, the fact that the energies of the peptide n–π^* transitions are close to those of the ^1L_a transitions would be expected to enhance the contributions arising from this mechanism. It should also be noted that, for the most part, these coupling interactions involving the tyrosine ^1L_a transitions and adjacent amide n–π^* and π–π^* transitions result in positive contributions to the ^1L_a rotatory strength, as one might expect on the basis of Woody's results with dipeptides.[61] Although many such interactions are not sufficiently strong to be among the principal coupling interactions of Table II, they nevertheless generally result in positive contributions to the rotatory strength of the tyrosine ^1L_a bands. A significant exception is tyrosine-115, where coupling between the ^1L_a and π–π^* transitions results in a negative contribution.

In many cases, the transitions which make positive contributions to the tyrosine ^1L_a rotatory strengths are the same ones which make negative contributions to the tyrosine ^1L_b bands. This reflects a change in the sign of the optical factor with a 90° change in the polarization of the tyrosine transitions. As an example, the ^1B_a bands of tyrosines-73 and -115 make significant positive contributions to the rotatory strength of the 240-nm band in RNase S while making sizable negative contributions to the rotatory strength of the 275-nm band.

Table II shows that there is a negative contribution to the rotatory strength of the tyrosine ^1L_a band as a result of coupling with the lower energy histidine bands. The interaction of histidine-105 with the ^1L_a transition of tyrosine-76, and histidine-119 with the tyrosine-73 ^1L_a transition, appears to make a significant negative contribution. This is not surprising, especially in the case of histidine-105, since this residue lies near tyrosine-76 in the crystal structure. However, the contribution to the rotatory strength arising from this interaction may be overestimated since both tyrosine-76 and histidine-105 are solvent accessible. Histidine-48 is in van der Waals contact with tyrosine-25, and as a result, there is a significant interaction between its lower energy transition and the ^1L_a transition of this tyrosine residue. A large positive contribution to the ^1L_a rotatory strength results.

As in the case of the ^1L_b transitions, it is possible that the tyrosine ^1L_a bands may undergo exciton-type coupling among themselves. In fact, the calculations predict a relatively small exciton effect for these transitions. They are predicted to give rise to a positive couplet, but the calculated splitting is quite small, approximately 1 nm. It is unlikely that the presence of such a couplet could be observed experimentally. The relatively large positive contribution which arises from the nondegenerate interactions of the ^1L_a transitions and the negative peptide Cotton effects that lie just to the blue would completely mask it.

The disulfide chromophores also make significant contributions to the circular dichroism of RNase S in the regions of the spectrum where the tyrosine ^1L_b and ^1L_a transitions occur. Cystine-40–95 has a negative inherent rotatory strength associated with its n_1–σ^* transition at 260 nm and a contribution of opposite sign which arises from the n_4–σ^* transition at 240 nm. The magnitude of the inherent negative rotatory strength at 260 nm is decreased as a result of coupling interactions with the ^1B_b and ^1B_a transitions of tyrosines-92 and -97, which result in positive contributions. Similar coupling interactions add to the positive inherent contribution to the rotatory strength of the n_4–σ^* band at 240 nm. Coupling with surrounding amide π–π^* transitions appears to make little contribution to the rotatory strength of either of the n–σ^* transitions associated with cystine-40–95.

As is obvious from Table III, the interaction of the degenerate n_1–σ^* and n_4–σ^* transitions of cystines-26–84, -58–110, and -65–72, which are not inherently optically active, with the ^1B_b and ^1B_a bands of tyrosines-73, -97, and -115 and with the π–π^* transitions of amides 71 and 108 makes a positive contribution to the rotatory strength at 250 nm. Coupling of the n–σ^* transitions of cystine-58–110 with the adjoining peptide π–π^* transition on alanine-109 makes a negative contribution. A negative rotatory strength contribution also arises from the interaction of the lower energy histidine transitions with the degenerate disulfide bands. This rotatory strength arises primarily as a result of a strong interaction between active-site histidine-119 and cystine-65–72.

(60) G. N. Ramachandran and V. Sasisekharan, *Adv. Protein Chem.*, **23**, 283–437 (1968); H. A. Scheraga, *Adv. Phys. Org. Chem.*, **6**, 103–184 (1968).

(61) R. W. Woody, *Biopolymers*, **17**, 1451–1467 (1978).

In summary, the negative ellipticity near 275 nm in the theoretical CD spectra of Figure 4 results from a negative tyrosine ^1L_b band near 275 nm in conjunction with a negative disulfide n_1–σ^* contribution near 260 nm. The predominant tyrosine contribution to this band arises from coupling of the ^1L_b transition on residue 73 with the higher energy B bands of residue 115, and vice versa. The overlap of the negative n–π^* peptide band with the positive tyrosine ^1L_a band at 225 nm makes a significant contribution to the positive ellipticity near 240 nm. Interactions involving coupling of tyrosine B bands and ^1L_a transitions make major contributions to the positive ellipticity at this wavelength. Disulfide bands at 240 and 250 nm also contribute to the positive ellipticity in this region. The magnitude of the positive band that appears to fall near 240–245 nm in the curves of Figure 4 is overestimated in comparison with its experimental counterpart. The extrema also appear to fall about 5 nm to the blue of the corresponding experimental band. These discrepancies probably result from the fact that a significant amount of ordered secondary structure was not included in the theoretical calculations. Such structure would be expected to induce the backbone amide transitions to give rise to a large negative Cotton effect just to the blue of the band in question, thus diminishing its magnitude and red shifting the apparent wavelength of the maximum.

Rotatory strength associated with the inherently dissymmetric disulfide of cystine-40–95 gives rise to negative ellipticity at 260 nm and positive ellipticity at 240 nm. The positive ellipticity that is calculated at 250 nm is contributed primarily from coupling of the degenerate n–σ^* transitions of the other three cystine residues with the B bands of the tyrosines.

The results of the calculations clearly indicate that the disulfides make significant contributions to the rotatory strength of RNase S in both the 275- and 250-nm regions. In fact, the data as summarized in Table IV indicate that the disulfides make larger contributions at both wavelengths than do the tyrosines. However, it should be pointed out that this distinction is at least to some extent artificial since the excited states of some of the tyrosine and disulfide transitions undergo considerable configuration interaction. This situation is reflected in the fact that the magnitude of the rotatory strength calculated for the 275–260-nm region is approximately the same whether or not the disulfides are included in the basis set.

The foregoing results clearly indicate that the Cotton effects which are associated with the side-chain chromophores of RNase S arise primarily from local interactions. As a result, they should be strongly dependent on the fine details of tertiary structure of all interacting chromophores in their immediate vicinity. Thus, they should serve as useful probes of tertiary structure at the microscopic level.

The changes in the experimental CD spectrum on going to higher pH may be accounted for as follows. As a result of X-ray structural data and chemical modification studies, it appears that tyrosines-73 and -115 are exposed to the solvent.[33,62,63] Titration of these residues to their phenolate forms should have the effect of increasing the absorption coefficient of the ^1L_b and ^1L_a transitions without appreciable change in the polarizations of the associated transition moments. In addition, both the ^1L_b and ^1L_a bands are red shifted upon titration to the phenolate anion. The increased intensity should also give rise to an increase in rotatory strength. Indeed, the 275-nm band in the CD spectrum of RNase S is red shifted and shows an increased negative ellipticity. The increased intensity and red shift of the ^1L_a transitions result in an increase in positive ellipticity in the 240-nm region. Thus, the titration curve of Figure 2b reflects the titration of tyrosines, and in all probability includes major contributions from residues 73 and 115.

A word may be in order with respect to the interaction of histidine transitions with the near-UV tyrosine and disulfide transitions. The calculations suggest that the histidines induce negative contributions to the rotatory strength of the tyrosine ^1L_a bands, and histidine-119 apparently makes a large negative contribution to the 250-nm disulfide band. However, no detectable change was observed in the 240–250-nm portion of the spectrum in the pH region corresponding to the titration of these histidine side chains. This result is not totally unexpected since protonation of the imidazole group probably causes only a relatively small change in the polarization of the transition moment associated with the lower energy histidine transition.[23] However, this would appear to infer that significant pH-dependent conformational changes of the histidine-119 side chain, similar to those suggested by Richards and Wyckoff,[33] are unlikely. Richards and Wyckoff have also reported movement of the histidine-119 side chain in the X-ray density maps of RNase S when various inhibitors are bound. If this motion occurs in solution, one might expect to see changes in the CD spectra of the enzyme in the presence of inhibitors. The CD difference spectrum reported in Figure 3 shows that there is a decrease in the ellipticity of the 275-nm band and an increase in the 240-nm band upon binding 3′-CMP. Thus, it appears likely that both the 240- and 275-nm Cotton effects could serve as possible probes for the putative motion of the histidine-119 side chain that has been suggested in proposed catalytic mechanisms.

Finally, it should be pointed out that the agreement between experiment and theory is really quite good, given the magnitude of the problem and the uncertainties associated with some of the data which were used in the calculations. Admittedly, the amplitude of the Cotton effect near 275 nm has been underestimated whereas the one near 240 nm has been overestimated. Nevertheless, there is at least semiquantitative agreement; the bands are of the correct sign, and the quantitative differences between experiment and theory, as revealed by comparison of Figures 1 and 4, are considerably less than one order of magnitude. Obviously, the situation could be made to appear even more favorable if the bandwidths of all of the transitions were treated as adjustable parameters in computing the theoretical curves of Figure 4.

Since these calculations were based upon atomic coordinates derived from X-ray-diffraction studies of crystals, the rather good agreement between experiment and theory would seem to indicate that there must be a considerable degree of similarity between the structures existing in the two states. This is made more significant by virtue of the fact that these results apply to the side-chain groups, where one might expect more marked deviations from the solid-state structure than within the peptide backbone. Although vibrational distortions certainly might be expected to occur, the average equilibrium structure which exists in solution must be quite similar to the one found in the crystalline state insofar as RNase S is concerned.

Acknowledgment. The support of the National Institute of General Medical Sciences of the National Institutes of Health through Grant GM-18092 is gratefully acknowledged. Equipment purchased with funds from Biomedical Sciences Support Grant S04-RR07099 was utilized in this research. We also thank F. M. Richards, H. G. Wyckoff, and T. Powers for kindly supplying us with atomic coordinates for ribonuclease S.

(62) R. W. Woody, M. E. Friedman, and H. A. Scheraga, *Biochemistry*, **5**, 2034–2048 (1966).

(63) H. W. Wyckoff, D. Tsernoglou, A. W. Hanson, J. R. Knox, B. Lee, and F. M. Richards, *J. Biol. Chem.*, **245**, 305–328 (1970).